1

Statistical modeling of extreme precipitation

CONTENTS

1.1 Introduction 1
1.2 Data characteristics 3
1.3 Univariate probability distributions for extreme precipitation .. 4
1.3.1 Block Maxima (BM) approach 4
1.3.2 Peaks over threshold (POT) approach 6
1.3.3 Nonasymptotic approach 8
1.3.4 Estimation methods 10
1.4 Intensity-Duration-Frequency curves 12
1.5 Regional Frequency Analysis 14
1.6 Nonstationarity and covariate modeling 16
1.6.1 Regression approach 16
1.6.2 Random effects and Bayesian regression 17
1.6.3 Detecting temporal nonstationarity 18
1.6.4 Statistical downscaling of extreme precipitation 18
1.6.5 Analysis of German heavy rainfall 20
1.7 Towards stochastic weather generator models 22
1.8 Conclusions and perspectives 26
Acknowledgement 27

1.1 Introduction

Precipitation intensities and frequencies are key variables for many environmental studies, not only limited to the field of hydrology but in many other fields, such as meteorology, climate sciences, and agronomy, and to the assessment of risks involving hydrometeorological processes, such as floods and droughts. Aggregate precipitation is the total amount of precipitation that accumulates over a specific period, typically measured as a height (of ac-

cumulated water) in millimeters (mm). As a result, there is very extensive literature proposing models for the distribution of precipitation at different temporal scales (sub-hourly, hourly, daily, monthly). For example, the most popular distribution used to model positive daily precipitation is probably the gamma distribution [79], which also generally provides an adequate fit for monthly precipitation thanks to its flexible shape, but the gamma distribution fails to capture heavy rainfall features at a high temporal scale, i.e. daily and sub-daily.

Modeling precipitation and its aggregates presents unique challenges compared to other weather variables, such as temperature. Precisely capturing the aggregation behavior of precipitation over time or space is crucial for many applications, including flood or drought risk assessment. This requires an explicit or implicit specification of an appropriate dependence model to combine the marginal distributions in time and space, where not only extreme but also moderate and low precipitation values can contribute to extreme aggregates. Another aspect specific to precipitation is its intermittence, which means that it is possible to observe many values of zero when a full observation series is considered. This requires considering the probability distribution as a mixture of a continuous component for positive precipitation and a discrete component at zero for the absence of precipitation.

While the entire distribution is important for precipitation, its extremes are of particular interest because of their impact on people through rain-induced floods [38], agriculture [99] and infrastructure [85]. The study of hydrological extremes was an important early application of extreme-value analysis [50, 55] and a catalyst for many methodological developments. Indeed, the use of a parametric model for the whole distribution can lead to significant bias in the estimates of the tail quantiles if the model is not properly specified. Therefore, it has become common practice to estimate tail quantiles of precipitation using models derived from Extreme-Value Theory [24, 8, 33].

This chapter reviews statistical approaches developed for studying some key aspects of precipitation extremes, but without any claim to be exhaustive. Section 1.2 provides a brief overview of typical data characteristics. Section 1.3 presents univariate probability distributions for modeling variability in extreme values and methods for estimating their parameters. Then, Section 1.4 demonstrates the application of these distributions in representing precipitation intensity or return values at different durations and frequencies. Section 1.5 explains how information can be aggregated spatially to obtain more efficient estimates of return values. The approaches in the aforementioned sections assume that extreme precipitation events are independent and identically distributed. However, there are various reasons to believe that this is not the case. For instance, seasonal and spatial patterns, as well as climate change, could induce nonstationarity. Section 1.6 reviews various approaches to detecting and modeling nonstationary precipitation extremes. The final section is a discussion presenting the concept of stochastic generators and emphasizing the importance of modeling extreme rainfall for simulation purposes.

This section examines the potential for stochastically generating synthetic yet realistic precipitation episodes across temporal, spatial, and spatiotemporal domains. For this purpose, we need generative models that can appropriately reproduce important statistical properties of extreme events but also of nonextreme events. In particular, such models must be able to adequately reproduce dependence across the domain. This chapter includes online supplementary material illustrating the practical applications of the discussed methods using real-world data.

1.2 Data characteristics

Precipitation is usually expressed in a unit of volume per area. It can be measured at the site of a rain gauge or determined by remote sensing at various spatial and temporal resolutions. In the former case, precipitation volume can be measured manually (typically once a day) or automatically with digital instruments, which allow obtaining time series with sub-daily measurements at relatively high frequency (*e.g.*, every minute). Often, the available stations with daily or more precise minute measurement frequencies differ by the length of their available time series, with more precise measurements being available only for more recent periods. The spatial coverage is also generally not uniform, typically being lower in areas that are difficult to access and sparsely populated. For analysis conducted at the global level, data availability is usually scarce in many low- and middle-income countries, especially in the Global South and the tropics [36].

Compared to gauging stations, remote sensing instruments such as weather radars or satellites can provide precipitation estimates at high spatiotemporal resolution [73]. However, due to their limited records in terms of temporal depth and the additional biases and uncertainties associated with remote sensing, the use of such precipitation data sets to fit extreme value models remains weakly explored.

Another potential data source is reanalysis data. Reanalysis combines past short-range weather forecasts with observations through data assimilation in numerical climate models. However, these data sets typically underestimate extreme precipitation events at local scales [34, 60], because they are available only at relatively coarse pixel resolution (*e.g.*, around 10km for standard reanalysis data products, such as ERA5). The value reported for a pixel can be viewed as an average taken over the whole pixel.

An example of the variety of available data is provided by the German Weather Service (Deutscher Wetterdienst, DWD). This service offers access to thousands of datasets of weather observations for Germany online at `https://opendata.dwd.de/climate_environment/`, in particular, daily precipitation but also observations with time steps of 1, 5, 10, 60 minutes. The

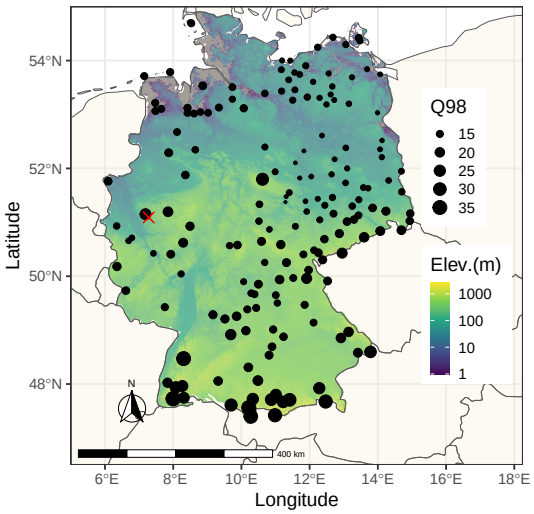

FIGURE 1.1
Map of precipitation gauges in Germany. Points are gauges with daily precipitation measurements for the period 1901–2023. The size of points reports empirical quantiles at level 0.98. The gauge at the location Neumühle (marked with a red cross) provides high-frequency data (1 minute) for the period 1975–2018. The color of the map background indicates elevation (in meter unit).

R package `rdwd` can retrieve this data, as demonstrated in the companion code provided in the online supplementary material. To practically illustrate some of the approaches discussed in this chapter, we use observations from 175 gauges in Germany for the period 1901–2023; see the map Figure 1.1 showing the topographic configuration of gauges and location-wise empirical precipitation quantiles at probability level 0.98.

1.3 Univariate probability distributions for extreme precipitation

Probabilistic methods describe the frequency and magnitude of extreme events of precipitation by modeling the upper part of the distribution, which is typically called the "tail". The main probabilistic methods are based on Extreme-Value Theory (EVT) used to analyze series of Block Maxima (BM; or Annual Maxima) and Peaks Over Threshold (POT; or Partial Duration).

1.3.1 Block Maxima (BM) approach

With this method, a time series of precipitation of a fixed duration is divided into subsets (*i.e.*, blocks) of the same length, usually by year, and the maximum value of each subset is extracted to obtain a sample of block maxima. The fundamental Fisher-Tippett-Gnedenko theorem [45, 49] states that, if the limiting distribution of the maxima of a properly normalized time series of independent and identically distributed observations exists, then it belongs to one of the following three distribution families: EVI (or Gumbel distribution), EVII (or Fréchet distribution), and EVIII (or reverse Weibull distribution). These three asymptotic distributions were combined by von Mises [114] and Jenkinson [59] into the Generalized Extreme-Value (GEV) distribution

$$G(y) = \exp\left\{ -\left[1 + \xi\Big(\frac{y-\mu}{\sigma}\Big)\right]_+^{-1/\xi} \right\}, \tag{1.1}$$

where $(a)_+ = \max(a, 0)$ and $-\infty < \mu < \infty$, $\sigma > 0$, $-\infty < \xi < \infty$. This distribution has three parameters: a location parameter μ, a scale parameter σ, and a shape parameter ξ, called the extreme-value index. With this parameterization, we denote the distribution as $GEV(\mu, \sigma, \xi)$ in the sequel.

The case $\xi = 0$ in (1.1) must be interpreted as the limit when $\xi \to 0$, which leads to the Gumbel distribution:

$$G(y) = \exp\left\{ -\exp\left[-\Big(\frac{y-\mu}{\sigma}\Big)\right] \right\}, \quad -\infty < y < \infty. \tag{1.2}$$

When $\xi > 0$, the GEV reduces to a Fréchet distribution and is said to be heavy-tailed. Conversely, when $\xi < 0$, the GEV distribution is the reverse Weibull distribution and has a finite upper bound of its support.

The motivation for modeling extreme precipitation properties often is to estimate the probabilities of rare events, especially high precipitation amounts, or, conversely, to estimate the amount or intensity of precipitation that can be expected to occur with a specific probability within a certain period. To achieve this, we can use the block maxima approach with the GEV distribution and obtain the necessary information by inverting equations (1.1) or (1.2). Using $G(q) = p$, we can derive the quantile function $G^{-1}(p) = q_p$ as

$$q_p = \begin{cases} \mu - \frac{\sigma}{\xi}\left\{1 - [-\log(p)]^{-\xi}\right\}, & \text{for } \xi \neq 0, \\ \mu - \sigma \log\left[-\log(p)\right], & \text{for } \xi = 0, \end{cases} \tag{1.3}$$

where q_p is the value that will not be exceeded with probability p within a block. Thus, for a block size of one year, p represents the annual nonexceedance probability. It is common to refer to return periods instead of annual probabilities, since statistically, the value of q_p can be expected to be exceeded on average once within the return period T, which is equal to $1/(1-p)$. It is worth noting that using return periods is only applicable in a stationary climate and

becomes difficult to interpret when the annual exceedance probability changes over time.

The asymptotic extreme value distribution brings a significant advantage in that it does not require knowledge of the parent distribution, making it widely used. Various studies have examined which of the three asymptotic distributions is most suitable for representing the statistical variability of maximum annual daily precipitation. The analysis of global and regional databases suggests that the EVII distribution (corresponding to heavy tails) is the most suitable for describing annual maxima of daily precipitation [94, 12, 80]. Working with block maxima has further advantages: intra-block dependence and nonstationarity do not have to be considered explicitly, and the delicate choice of certain tuning parameters (e.g., thresholds in the peaks-over-threshold approach described in the following section) is avoided. In some cases, only historical maxima data is available, and the BM approach directly exploits this information; see, e.g. [61]. Finally, maxima data may have undergone more thorough quality checking than the original data available at higher temporal resolution; see, e.g., [88].

1.3.2 Peaks over threshold (POT) approach

The benefits of the BM method highlighted previously come with a downside. Shortcomings include the loss of information (as only a maximum of each year is retained) and questionable asymptotic assumptions when effective sample sizes are relatively small, *e.g.*, due to only a few independent precipitation episodes during a year, or due to strong seasonalities, such that most annual maxima occur during a specific season. Moreover, intra-block behavior (e.g., serial dependence and seasonal patterns) cannot be inferred from maxima data. The peaks-over-threshold approach can provide more flexibility and alleviate such problems.

The Generalized Pareto distribution is commonly used to study those components of a series that exceed a high fixed threshold value, as suggested by the Pickands-Balkema-de Haan [6, 96] theorem. Under the same conditions as those of the Fisher-Tippett-Gnedenko theorem, the conditional distribution of Y above a threshold u, $\Pr(Y \leq u+z \mid Y > u)$, converges to the Generalized Pareto (GP) distribution, denoted H, as u tends to infinity:

$$H(z) = 1 - \left(1 + \xi \frac{z}{\tilde{\sigma}}\right)_+^{-1/\xi}, \tag{1.4}$$

with $-\infty < \xi < \infty$ and $\tilde{\sigma} > 0$.

Note that the special case $\xi = 0$ has to be interpreted as a limit, in analogy with the GEV case $\xi = 0$, viz.,

$$H(z) = 1 - \exp\left(-\frac{z}{\tilde{\sigma}}\right), \quad z > 0, \tag{1.5}$$

which corresponds to an exponential distribution with rate parameter $1/\tilde{\sigma}$.

The parameters of the GP distribution of threshold excesses are uniquely determined by those of the associated GEV distribution of the block maxima. In particular, the shape parameter ξ in (1.4) is equal to that of (1.1), and its interpretation is the same as for the GEV distribution (*e.g.*, if $\xi > 0$, then the GP distribution is heavy-tailed). The relationship between the scale parameters of the GEV and GP distributions is $\tilde{\sigma} = \sigma + \xi(u - \mu)$.

Using (1.4) and (1.5), return levels of the parent distribution of Y for $y > u$ can be derived from

$$\Pr(Y \leq y) \approx \begin{cases} 1 - \lambda_u \left[1 + \xi \left(\frac{y-u}{\sigma}\right)\right]_+^{-1/\xi}, & \text{for } \xi \neq 0, \\ 1 - \lambda_u \exp\left(\frac{y-u}{\sigma}\right), & \text{for } \xi = 0, \end{cases} \tag{1.6}$$

where $\lambda_u = \Pr(Y > u)$ can be estimated empirically as the proportion of the data exceeding the threshold u. Solving $\Pr(Y \leq y_p) = p$, we obtain

$$y_p \approx \begin{cases} u + \frac{\sigma}{\xi}\left[\left(\frac{1-p}{\lambda_u}\right)^{-\xi} - 1\right], & \text{for } \xi \neq 0, \\ u + \sigma \log\left(\frac{1-p}{\lambda_u}\right), & \text{for } \xi = 0. \end{cases} \tag{1.7}$$

However, it should be noted that these relationships are still considered asymptotic. Two central assumptions are made when using this procedure in practice. First, the asymptotic argument must be valid for the parent distribution $F_Y(\cdot)$ of precipitation; second, an appropriate threshold u must be found such that the GP model provides a good approximation to exceedances of u.

To detect an appropriate threshold u to fit a GP distribution, a variety of methods exist, see [103, 68] for reviews. In an extensive application of various methods to 1714 gauges with over 110 years of available daily precipitation observations from the NOAA-NCDC database (in open access), [68] found that graphical methods [24] and goodness-of-fit metrics based on asymptotic properties of the GP distribution performed best. We conclude by mentioning that there have been recent advances for this issue [115, 86, 81] that would deserve a more widespread application to precipitation data.

Apart from threshold selection, another difficulty of the POT approach is the assumption of independence in data series. In a worldwide assessment, the series of daily precipitation of the stations belonging to the Global Historical Climatology Network (GHCN) were shown to present significant autocorrelation, which becomes weaker for threshold exceedances when increasing the threshold value [35]. Temporal dependence between successive time steps becomes stronger for sub-daily rainfall time series, and extreme events tend to occur in clusters more often.

One common approach to handling clusters of extremes is declustering. Once a definition of clusters has been decided, the maximum excess in each cluster is recorded, and these cluster maxima are then assumed to be independent [30, 44]. The GP distribution can then be fitted to these independent cluster maxima. Defining clusters is problematic since the method is sensitive

to how exactly a cluster is defined, *i.e.*, often based on threshold and run length selection. Again, as with the block maxima approach, there is a substantial waste of information by only considering the maximum of each cluster in the modeling procedure.

[42] proposed to fit the GP distribution with the incorrect assumption of independence between exceedances of a high threshold. They use all threshold exceedances in the modeling procedure, dealing with the problem of dependence through other methods. This approach significantly reduces bias in parameter and return level estimates, but it also underestimates standard errors associated with model parameters due to the incorrect assumption of independence. To address this issue, the authors utilize a method developed by [105], which enables the adjustment of the standard errors through a relatively simple modification.

1.3.3 Nonasymptotic approach

Hosking and Wallis [54, Chapter 5] proposed using alternative distributions, in addition to the GEV distribution, for modeling annual maxima. They argue that the requirements for approximating the distribution of annual maxima with a GEV distribution are often not satisfactorily met for variables such as precipitation.

The Generalized Logistic (GL), Generalized Normal (GN), and Pearson type III (P3) distributions, proposed by Hosking and Wallis [54, Chapter 5], are potential candidates with three parameters μ, σ and ξ, and are recalled below.

Generalized Logistic

$$F(y) = \begin{cases} \dfrac{1}{1 + \left(1 + \xi \frac{y-\mu}{\sigma}\right)_+^{-1/\xi}}, & \text{for } \xi \neq 0, \\ \dfrac{1}{1 + \exp\left(-\frac{y-\mu}{\sigma}\right)}, & \text{for } \xi = 0. \end{cases}$$

Generalized Normal

$$F(y) = \begin{cases} \Phi\left(\log\left(1 + \xi \frac{y-\mu}{\sigma}\right)_+^{1/\xi}\right), & \text{for } \xi \neq 0, \\ \Phi\left(\frac{y-\mu}{\sigma}\right), & \text{for } \xi = 0, \end{cases}$$

where $\Phi(y)$ is the standard Normal distribution.

Pearson type III or generalized gamma distribution

$$F(y) = \begin{cases} \dfrac{\gamma\left(4/\xi^2, 2\frac{y-\mu}{\sigma} + 4/\xi^2\right)}{\Gamma\left(4/\xi^2\right)}, & \text{for } \xi > 0, \\ \Phi\left(\frac{y-\mu}{\sigma}\right), & \text{for } \xi = 0 \\ 1 - \dfrac{\gamma\left(4/\xi^2, -2\frac{y-\mu}{\sigma} - 4/\xi^2\right)}{\Gamma\left(4/\xi^2\right)}, & \text{for } \xi < 0, \end{cases}$$

with support $\left\{y : [2(y-\mu)/\sigma + 4/\xi^2]\xi > 0\right\}$ where $\gamma(\alpha, t)$ is the lower incomplete gamma function, *i.e.*, $\gamma(\alpha, t) = \int_0^t s^{\alpha-1}\exp(-s)ds$, and $\Gamma(\alpha) = \lim_{t\to\infty}\gamma(\alpha, t)$.

Table S2 in the Supplementary material of [35] presents recent references that use a range of probability distributions to represent annual maxima of daily precipitation. Although these other distributions have been identified empirically as suitable for modeling annual precipitation with specific datasets, it is important to note that there is no general asymptotic justification for them. Violating the asymptotic theory may cast doubt on the ability of the fitted models to extrapolate to low-probability events and high-return periods.

The applicability of classical EVT to annual maxima of precipitation, both for daily and shorter durations, has also been questioned by Veneziano and coauthors [110, 111]. They offer an alternative approach to dealing with rainfall extremes and present a unified asymptotic theory of rainfall extremes, which includes annual maxima, excesses above high thresholds, and intensity-duration-frequency curves. The analysis is based on stationary multifractal representations of rainfall and extends the familiar results from EVT [111].

The need to overcome some limitations of classical EVT due to the paucity of data led to the development of alternative approaches that allow for more efficient use of the available data to infer the distribution of extremes.

One approach is based on so-called compound distributions and has recently been proposed for hydrological applications by [77]. They introduce the Metastatistical Extreme Value Distribution (MEVD in the following, not to be confounded with Multivariate EVDs). The starting point is still the consideration of the distribution of the maximum M_n on n independent and identically distributed random variable Y_i, $i = 1, ..., n$, inside a block. However, instead of considering the limit distribution of the normalized sequence M_n, they consider the non-asymptotic distribution, namely

$$\Pr(M_n \leq y) = [F(y;\theta)]^n$$

where $F(\cdot;\theta)$ is the parametric distribution of Y_i, *i.e.*, the parent distribution. The MEVD treats as random variables both the number of events per block n in each year and the parameters θ. The resulting distribution is the compound distribution

$$G(y;\lambda) = \int \sum_{n=1}^{\infty} [F(y;\theta)]^n p(n;\lambda)\pi(\theta;\lambda)\mathrm{d}\theta$$

where $p(n;\lambda)$ is the 'a priori' probability distribution of the number of events per block, $\pi(\theta;\lambda)$ is the 'a priori' distribution on θ, and λ represents a vector of suitable prior hyperparameters. For practical applications, the MEVD is

approximated by

$$\widehat{G}(y) = \frac{1}{J}\sum_{j=1}^{J}[F(y;\widehat{\theta}_j)]^{n_j}$$

where J is the number of blocks of observations, n_j is the number of wet events in the jth block and $\widehat{\theta}_j$ is the estimate previously obtained within each block by considering the distribution $F(\cdot;\theta)$.

This two-step procedure does not account for the variability associated with the different estimates $\widehat{\theta}_j$. To overcome this limitation, [129] propose to rewrite the compound distribution as a hierarchical model and fit it under a Bayesian framework. Another potential problem in the model specification is the assumed independence of the event. This is especially true when we consider sub-daily data. Finally, in modeling daily rainfall, [77] chose the Weibull distribution, claiming the superiority of this distribution over other distributions. Another widely used distribution is the gamma distribution. However, both distributions are within the domain of attraction of the EVI (Gumbel) distribution. In terms of the asymptotic behavior of the distributions, this fact contradicts the common use of the EVII (Fréchet) distribution in modeling daily annual maxima [94, 12, 80].

The approach described above relies on expert knowledge of the hydrological community about the statistical distribution of precipitation. Chapter **??** discusses other approaches that model the bulk of the data and the tails together, and that extend the EV distributions by broadening the range of extreme value limit distributions.

1.3.4 Estimation methods

Various estimation methods are currently used to fit the above models for heavy precipitation analysis; for a recent review, see [84]. Among the numerous options, two are particularly popular among hydrologists: the maximum likelihood (ML) method and a method based on Probability Weighted Moments (PWMs).

Although there is no clear superiority among different methods, the ML method can generally be considered the most efficient approach for large sample sizes, as long as the model is not misspecified. Computational details on ML estimation of μ, ξ, σ in the GEV model are presented in [97] and Chapter **??**. Another advantage of ML is that the method can be readily adapted to extreme-value models with covariates, see §1.4 and §1.6.1.

The PWM estimation method is a widely used and relatively robust alternative to the ML approach, particularly when the sample size is small [48]. The PWM of a random variable Y is defined as

$$\mu_{p,r,s} = \mathrm{E}[Y^p\{F(Y)\}^r\{1-F(Y)\}^s],$$

where p, r, and s are real numbers, provided that the expectation exists.

The conventional definition of moments corresponds to the case $r = s = 0$. The estimation method involves matching the PWMs of a random variable Y with their empirical versions, similar to the classical method of moments. The special case $p = 1$ and $s = 0$ is widely used and we denote $\beta_r = \mu_{1,r,0}$. The unbiased estimators of β_r is given by

$$\hat{\beta}_r = \frac{1}{n} \sum_{j=r+1}^{n} \left(\prod_{i=1}^{r} \frac{j-i}{n-i} \right) Y_{j:n},$$

where $(Y_{1:n}, \ldots, Y_{n;n})$ represents the ordered sample [67].

For the GEV distribution, [55] show that we can get an explicit formula for β_r, namely,

$$\beta_r = \frac{1}{r+1} \left[\mu - \frac{\sigma}{\xi} \left\{ 1 - (r+1)^{\xi} \Gamma(1-\xi) \right\} \right], \quad \xi < 1 \text{ and } \xi \neq 0,$$

which leads to the PWM estimation when these moments are matched. Explicit formulas of β_r, $r = 0, 1, 2$ are also available for the GP distribution [117]. In both cases, a constraint is placed on the shape parameter of the GEV or GP distribution (e.g., $\xi < 1$). [25] proposed a penalized maximum likelihood (PML) approach with $\xi < 1$, which outperformed the PWM in terms of bias and mean square error for parameter and quantile estimations.

The L-Moments (LMs) estimation method is another popular method. It is based on the rth L-moments, namely

$$\lambda_r = \frac{1}{r} \sum_{k=0}^{r-1} (-1)^k \binom{r-1}{k} \mathrm{E}(Y_{r-k:r}).$$

They have similar properties as PWMs since they are defined as linear combinations of them [54, Equation 2.36], namely

$$\lambda_{r+1} = \sum_{k=0}^{r} (-1)^{r-k} \binom{r}{k} \binom{r+k}{k} \beta_k.$$

L-moments, however, are more convenient because they are more directly interpretable as measures of the scale and shape of probability distributions [53]. In particular, two dimensionless versions of L-moments, the L-moment ratios

$$\tau_r = \frac{\lambda_r}{\lambda_2}, \qquad r = 3, 4,$$

measure the shape of a distribution independent of the scale of measurement. They are called L-skewness and L-curvature, respectively [54].

We conclude this section by noting that the recent software review [9] provides a catalog of existing packages in the R software, where the implementations of the estimation methods are compared and numerical issues of practical importance are highlighted. An example of the application of estimation methods using such packages to annual maxima of

daily precipitation can be found in the online supplementary material, see `github.com/cgaetan/Handbook-on-Statistics-of-Extremes-Chapter25`.

1.4 Intensity-Duration-Frequency curves

Intensity-Duration-Frequency (IDF) curves illustrate the relationship between the intensity and duration of precipitation at different return periods. These curves are useful in engineering applications for estimating the risk of failure when designing infrastructure such as urban drainage networks, pumping stations, wastewater treatment plants, and retention basins.

Let $R(d)$ be the total amount of precipitation in a time interval of length d (duration). For example, $R(60)$ is the hourly amount of precipitation if precipitation is recorded every minute. This quantity $R(60)$ divided by 60 gives the amount of precipitation per time unit. The annual maxima of this quantity is denoted by $I(60)$ and more generally such annual maxima intensities are denoted $I(d)$. IDF curves typically consider $I(d)$ but approaches based on exceedances above a threshold or based on the entire distribution have also been proposed [51].

The T-year return level of $I(d)$ is given as

$$i(T, d) = F_d^{-1}\left(1 - \frac{1}{T}\right) \tag{1.8}$$

where F_d is the distribution of the annual maxima $I(d)$. Finally, IDF curves are logarithmic plots of $i(T, d)$ against duration d, for different fixed values of T. Figure 1.2 shows an example for annual precipitation intensity maxima at station Neumühle (Germany; see Figure 1.1) at durations $d \in \{1\text{min}, 4\text{min}, 8\text{min}, 16\text{min}, 32\text{min}, 1\text{h}, 2\text{h}, 4\text{h}, 8\text{h}, 16\text{h}, 1\text{d}, 2\text{d}, 3\text{d}, 4\text{d}, 5\text{d}\}$ for the period 1975-2018. For a code that reproduces the figure, see the online supplementary material.

In the traditional approach for estimation of IDF curves from data, the first step is to calculate the annual block maxima $I(d_k)$ at specified durations d_k, $k = 1, \ldots, K$ and fitting one of the previous parametric distributions for the maxima, namely $F_d(\cdot|\theta(d_k))$, with parameter vector $\theta(d_k)$. Then, the IDF curves are obtained in two sequential steps, where one: (a) uses (1.8) to obtain estimates of $i(d, T)$ for different combinations of (d, T), and (b) uses the estimates obtained in (a) to regress a parametric relationship of a separable function of d and T, *i.e.*,

$$i(T, d) = \frac{a(T)}{b(d)} \tag{1.9}$$

where $a(\cdot)$ and $b(\cdot)$ are positively valued functions; see, *e.g.*, [63].

The Equation (1.9) expresses that precipitation intensity decreases as duration increases, for a given return period. The separability hypothesis has an

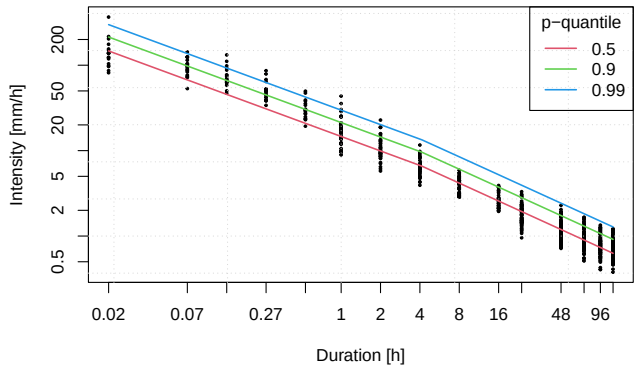

FIGURE 1.2
IDF curves for annual maxima of precipitation intensity (black points) at station Neumühle (Germany) (1975-2018). The IDF curves are estimated using the independence likelihood (1.11) for the model (1.10).

important effect on the distribution of $I(d)$. In fact, we can see that $a(T)$ is the T-year return level of the scaled intensities $I = b(d)I(d)$ that are independent of d, or equivalently, we can suppose that

$$I(d) \stackrel{d}{=} \frac{1}{b(d)} I,$$

where I is a random variable with T-year return level $a(T)$.

This approach is referred to as a semi-parametric approach because $a(T)$ is derived by fitting a pre-specified distribution model to the entire sample of the scaled intensities $b(d_k)I(d_k)$, $k = 1, \ldots, K$. [63] proposed a mathematical formula for $b(d)$, namely

$$b(d) = (d^\nu + \psi)^\eta, \quad \text{with } \eta, \nu, \psi \geq 0 \text{ and } \nu\eta \leq 1.$$

Empirically, they postulate that the assumption $\nu = 1$ is a sufficiently good approximation, resulting in a two-parameter IDF model. If the scaled intensity is such that $I \sim GEV(\mu, \sigma, \xi)$ then $I(d) \sim \text{GEV}(\mu(d), \sigma(d), \xi(d))$ with

$$\mu(d) = \mu\sigma(d+\psi)^{-\eta}, \tag{1.10a}$$
$$\sigma(d) = \sigma(d+\psi)^{-\eta}, \tag{1.10b}$$
$$\xi(d) = \xi. \tag{1.10c}$$

In such a case the distribution is termed duration-dependent GEV (d-GEV) distribution [63], which enables describing the annual maxima of all durations simultaneously. Equations (1.10) assume a scaling that is independent of the

return period. The d-GEV model can be extended relatively straightforwardly to relax this assumption, see [41] for an example. Nonstationary general IDF relationships can also be incorporated by allowing the location parameter μ and scale parameter σ to depend on time-varying or space-varying covariates. An example of these models can be found in [91].

The estimation of the parameter for d-GEV is complicated by the dependence that usually exists between the maxima of different durations within one year.

One option to tackle this issue is to utilize an independence likelihood approach [21]. The likelihood is constructed as if the maxima of intensity to different durations d_k, $k = 1, \ldots, K$ within a year, t were independent. Assuming that the observations over n years are independent, the logarithm of the independence likelihood is

$$\ell(\mu, \sigma, \xi, \psi, \eta) \quad = \quad \sum_{t=1}^{n} \sum_{k=1}^{K} \log f(I_t(d_k); d_k, \mu, \sigma, \xi, \psi, \eta), \tag{1.11}$$

where $f(\cdot; d, \mu, \sigma, \xi, \psi, \eta)$ is the density function of GEV$(\mu(d), \sigma(d), \xi)$ distribution. The estimation procedure is currently implemented in the R package IDF. The estimates are unbiased according to estimation theory; however, since the standard errors given for the parameters are based on a pseudo-likelihood, they are generally too small. A correction to take into account the dependence among the durations can be found in [21, Eq. (8)]. The IDF package in its current implementation should be used when the aim is merely to provide pointwise quantile estimates.

[82] investigated the structure of models for ordered multivariate extremes. They showed that the inequalities

$$\max_i R_i(d) \leq \max_i R_i(d') \leq \frac{d'}{d} \max_i R_i(d),$$

with d' a multiple of d, restrict the marginal distribution, namely $\xi(d) < 0$, and $\xi(d') \geq 0$ or $\xi(d) = \xi(d') \geq 0$. In the analysis of real precipitation data, the last case is most often observed and entails $\sigma(d)(d/d') \leq \sigma(d') \leq \sigma(d)$ and $\mu(d)(d/d') \leq \mu(d') \leq \mu(d)$. Such results justify the adoption of equations (1.10). Moreover, [82] suggested using a multivariate extreme value distribution for I_t.

For interpolation and extrapolation to unobserved durations d, [109] suggest using a Brown–Resnick max-stable process [17] $\{I(d), d \in D\}$, where $D \subset \mathbb{R}_+$ represents the continuous space of the different durations. One potential criticism is that the Euclidean distance in duration space does not provide an adequate distance measure and that it leads to different dependence characteristics for shorter durations compared to longer durations, such that further adjustments in the dependence structure, such as using nonstationary dependence, would be appropriate.

1.5 Regional Frequency Analysis

The primary goal of Regional Frequency Analysis (RFA) is to estimate the return period of extreme hydrological events at a network of locations when there is only limited or no hydrological data available. To achieve this goal, the first step is to identify a homogeneous region to identify measured locations that are similar to the site of interest [54]. The second step is to pool the spatial information for regional estimation.

More precisely, given geographic space $\mathcal{S}$, a homogeneous region, say $\mathcal{R}$, is defined as a set of sites $s \in \mathcal{S}$ where the distributions of the precipitation $Y(s)$ are equal up to a normalizing factor, *i.e.*,

$$\mathcal{R} = \left\{ s \in \mathcal{S} : Y(s) \stackrel{d}{=} \sigma(s) Z \right\},$$

where $\stackrel{d}{=}$ means equality in distribution and Z is a positively-valued random variable. The cdf of Z is called the regional cdf.

There exists a wide variety of methods that attempt to find homogeneous regions (see [54, 106] for two reviews), but no consensus on the best procedure has yet been reached, since all approaches exhibit certain advantages and limitations; *e.g.*, regions determined based solely on geographic proximity criteria may not guarantee hydrological or climatological similarity. Purely objective criteria based solely on minimization of heterogeneity dissimilarities may lead to fragmented regions, whereas subjective expert-based partitioning may be unfeasible in the case of large observational networks.

After identifying a homogeneity region, tests are performed among the sites based on the empirical estimates of the L-moments (see again [54], for the mathematical definition of these tests). The significance levels of the tests are obtained under the parametric assumption that precipitation follows a kappa-like distribution.

[70] suggest identifying distinct homogeneous regions based on the upper tail similarity. A ratio of PWMs (or equivalently of L-Moments), defined as

$$\omega = \frac{3\beta_3 - \beta_0}{2\beta_1 - \beta_0} - 1 = \frac{1}{2}\left(1 - \frac{\lambda_3}{\lambda_2}\right) = \frac{1}{2}\left(1 - \tau_3\right)$$

summarizes the upper tail behavior for each station. It is possible to show that

$$\omega_{GEV} = \frac{3^\xi - 1}{2^\xi - 1} - 1, \qquad \omega_{GP} = \frac{5 - \xi}{3 - \xi} - 1$$

if Z follows a GEV distribution or a GP distribution, respectively. Comparing two values of $\omega(s_i)$ and $\omega(s_j)$ estimated at two different sites s_i and s_j provides a simple dissimilarity measure that does not depend on the scale factor. [70] consider the distance $d_{ij} = |\omega(s_i) - \omega(s_j)|$. If the distance is close to zero, it means that the two locations have similar (up to a rescaling constant)

marginal distributions. This dissimilarity measure can be used in a clustering algorithm.

Finally, similar to the classical RFA approach, the regional parameters can be estimated by pooling all station data from the same cluster.

1.6 Nonstationarity and covariate modeling

The distribution of precipitation can vary over space, time, and along other covariates. Variation over time can occur at different temporal scales, including diurnal, seasonal, and long-term climate-change patterns, and the distribution can depend on spatial position through orographic variables, such as elevation. Numerous climate-change studies have investigated the detection of long-term temporal trends in precipitation extremes. For example, by using temperature as a covariate, it has been intensively explored how precipitation, and especially extreme precipitation, scales with temperature, and whether the relationship follows the scaling property of the Clausius–Clapeyron formula derived from physical laws [74, 72, 118, 92, 71, 125, 46]. Results indicate that the relationship appears to depend quite strongly on the specific properties of the regional climate system; the positive scaling suggested by the physical equation was confirmed for various regional contexts, although with estimated scaling parameters that may significantly deviate from the one suggested by the equation.

In practice, we often try to determine if there is a trend in the distribution of precipitation, in particular in its extremes, and if so, to quantify it more precisely. A common approach to assess such trends consists of statistical regression, where we incorporate appropriately chosen covariates into the parameters of one of the probability distributions appropriate for extreme precipitation. A general review of statistical regression is provided in Chapter **??**.

Nonstationarity can also be introduced in the spatial dependence structure of generative models for extreme precipitation, as achieved by [19, 20, 128]; see §1.7.

1.6.1 Regression approach

The regression approach consists of modeling precipitation and its extremes conditional on covariates, which are used to construct a predictor for one or several parameters of the probability distribution of a response variable defined from precipitation, such as maxima or threshold excesses. Different functional forms (e.g., linear, nonlinear, with or without interaction terms of several covariates) are possible to construct and estimate the predictor from available covariates. In some cases, it may be useful to include random variables (also called random effects) in the predictor to account for sources of

precipitation variability not well explained by the available covariates; this approach requires handling latent variables and is discussed separately in §1.6.2. Regression is often used to study the response of precipitation extremes to other variables in the climate system to allow for physical interpretation, especially for explaining local precipitation behavior through large-scale climate conditions, while keeping track of the uncertainties involved in the estimated covariate effects and predictions of the response.

A standard approach for regression modeling of precipitation extremes consists of including covariates into the three parameters (μ, σ, ξ) of the GEV distribution of block maxima as proposed by [22], or in the two parameters $(\tilde{\sigma}, \xi)$ of the GP distribution of positive excesses above a high threshold. Various `R` implementations of generalized linear GEV and GP models are available in standard extreme-value packages. The `evgam` package [123] provides a very comprehensive implementation of Generalized Additive Models (GAMs) , allowing for nonlinear covariate influence with automatically estimated smoothness of the predictor functions. `evgam` also implements quantile regression, useful to estimate a nonstationary high threshold for peaks-over-threshold regression with the GP distribution, via the Asymmetric Laplace response distribution. Use of `evgam` for precipitation extremes will be illustrated in the real data example in §1.6.5.

1.6.2 Random effects and Bayesian regression

In the Bayesian setting, expert knowledge can be elicited to set informative prior distributions for important model parameters. A common approach is to model trends and dependence across space and time by using a latent Gaussian process that can be viewed as a random effect capturing precipitation variability that cannot be deterministically explained by other covariates; it is embedded into one or several of the parameters of a univariate response distribution, such as the GEV for maxima or the GP distribution for threshold excesses. As is usual for Bayesian hierarchical models, observations are assumed to be conditionally independent of the latent process.

[26] have pioneered this approach using Markov-Chain Monte-Carlo inference for modeling spatial variability and uncertainty in precipitation extremes by using the GP distribution for threshold excesses and a binomial distribution for the number of exceedances at each observation location. A similar model but using the fast and accurate deterministic Laplace approximations available through the method INLA (Integrated Nested Laplace Approximation) was proposed by [89]. [100] develop spatial MCMC inference with the GEV distribution. [27] carry out an application where the tail index ξ is also allowed to vary across space, in contrast to most other works where the tail index is kept constant, which may be beneficial in terms of computational cost and interpretation. [101] proposed a modification of such models where the conditional independence assumption, which implies unrealistic small-scale behavior of the model, is dropped. Finally, [52] used a large dataset of satellite-derived

precipitation data and showed how spatial trends in excesses above a high threshold can be flexibly modeled by embedding spatial Gaussian processes into the parameters of the point-process likelihood for univariate extremes by using the so-called "Max-and-Smooth" approach.

1.6.3 Detecting temporal nonstationarity

Formal decision tools for detecting temporal nonstationarity can be used to assess the presence of seasonal cycles and long-term effects, for example climate change effects. A common approach is to use the aforementioned regression techniques by including time, or a time-varying variable such as large-scale temperature in the context of climate change, as a covariate, such that significant effects of this covariate can be viewed as a formal proof of nonstationarity. Default confidence bounds provided by regression software are usually based on the assumption of conditional independence of observations given covariates, which could be violated when modeling precipitation data, such that significance levels could be biased. A solution for the issue of temporal correlations in extremes is to work with annual maxima or with declustered threshold exceedances. Alternatively, block bootstrap approaches with temporal blocks (*e.g.*, years) could be used to obtain more reliable confidence bounds for regression parameters under the null hypothesis of no influence of the covariate on the response.

In climate change studies, it is often desirable to show significant changes over an entire region rather than just for a single weather station, which requires accounting for spatial autocorrelation and can increase the statistical power to detect changes. Whereas methods such as field-significance tests [75] are based on combining results from locationwise statistical tests, more recent approaches propose using a dependence model from spatial extreme-value theory, such as max-stable processes, to join the marginal distributions, into which regression parameters have been included to detect a temporal slope [119].

A model-free standard approach for detecting monotonic trends in a time series of independent observations is the Mann–Kendall (MK) test [76], a widely applied, simple, and robust statistical test for identifying climate-change effects based on resampling of data series through permutation of the time index. The test has also been adapted to dependent series by first extracting independent residuals obtained from fitting a time series model, but this modification can alter the performance of the test [124]. A simple approach for precipitation extremes consists of extracting yearly maxima before applying the MK test, for example done by [23, 127]. [65] reviews various other trend detection techniques for hydrological data, most of them checking for significance in some correlation measure between the observed precipitation value and the time of observation.

1.6.4 Statistical downscaling of extreme precipitation

The procedure of statistical downscaling consists of using a statistical transfer method, such as a regression model, that transforms input data available at a relatively coarse resolution (large scale) to a simulation or probability distribution of a target variable at a finer resolution (local scale). Large-scale data could consist of climate model output or satellite measurements of precipitation and potentially other useful predictor variables available at relatively large spatial and atmospheric scales. Typically, such large-scale data can be interpreted as an average value over a voxel, *i.e.*, over the cube defined as the Cartesian product of a spatial pixel and a time interval. In the setting of reanalysis where observational data has been assimilated into a numerical climate model, such large-scale data can be considered as a proxy for the average of real weather in the voxel. The local-scale data is typically given by precipitation observed at rain gauges, *i.e.*, it is point-source data. Parameters of the transfer function are calibrated using historical data jointly available at both scales, and the fitted transfer function can then be applied for downscaling large-scale data, *i.e.*, for producing local-scale data over areas and periods where local-scale data is not available. An example would be future local-scale projections of precipitation, since typically only large-scale climate-model simulations of precipitations and other atmospheric variables are available.

Some approaches explicitly model the spatial and/or temporal autocorrelation at the local scale to precisely guide the disaggregation of the large-scale averages into small-scale values. A special case of downscaling is the temporal disaggregation of two types of precipitation data available at the same spatial scale but with different temporal scales. Here, the goal would be to disaggregate cumulative precipitation available for relatively large time steps (*e.g.*, daily) to smaller time steps (*e.g.*, hourly) [2].

A standard regression approach to downscaling is to work with an asymptotic distribution for threshold excesses of precipitation at the local scale and to include large-scale precipitation (and potentially other predictors) from pixels near the local-scale coordinate [47]. In general, downscaling techniques allowing for nonlinear transfer functions, such as GAMs, tend to perform better, as highlighted by [108] in a detailed study of downscaling river flows. Downscaling of precipitation with coherent spatial patterns for areas where no local-scale data was available could be done in different ways. For example, [7] study downscaling of location-wise annual maxima of precipitation and compare different approaches that combine two steps: first, downscaling from the large-scale data to the local-scale univariate distributions for locations s with available data; second, spatial interpolation of the downscaled univariate values. They find that spatial conditional simulation based on a max-stable process with a parametric dependence structure improves accuracy as compared to more traditional, simpler interpolation schemes. [87] consider the setting where local-scale data are available on a regular and dense grid, and work under the assumption of a physical constraint where the large-scale value

must be equal to an average of small-scale values. They implement spatial disaggregation of max-stable processes where the large-scale values constrain the stochastic simulation of the local-scale values. Then, it is possible to sample from the spatial distribution of local-scale values in situations where only large-scale data are available.

1.6.5 Analysis of German heavy rainfall

We illustrate regression modeling to capture spatial and temporal patterns in the marginal distributions of extreme daily cumulated precipitation using observation data from gauges in Germany during the period 1901–2023, as shown in Figure 1.1 and detailed in §1.2. Precipitation often shows strong spatial trends, as already suggested by the spatial patterns arising in the high empirical quantiles reported on the map. Some gauges available in the Alpine region below latitude 48° were removed during data preprocessing since precipitation regimes in this area are expected to be quite different from flatter regions in the rest of Germany.

We explore GEV models for annual maxima and GP models for excesses (without declustering) above a high threshold fixed to an estimated quantile at level 0.98, using the `evgam` package of the `R` software. Covariates included here are longitude, latitude, and year of observation. To maintain simplicity in models and interpretation, here we do not use other covariates (e.g., elevation or temperature) that would be available in principle and could allow for interesting physical interpretations of the drivers of the variability in observed precipitation; see, e.g., [128] who model threshold exceedances of precipitation, as well as their dependence, for several large river catchments by using regional temperature averages as covariate.

We follow common practice in extreme-value regression and do not let the shape parameter ξ vary with covariates, which helps to achieve numerical stability of estimation and model parsimony and facilitates interpretation. Daily observations are denoted by Y_i with the index $i = 1, \ldots, n$ running through all combinations of days and locations with observations. Locations are identified by their longitude-latitude coordinates $(\mathrm{lon}_i, \mathrm{lat}_i)$. We denote the observations of annual maxima by $M_k = M(\mathrm{lon}_k, \mathrm{lat}_k, \mathrm{year}_k)$, and for the observed positive threshold exceedances, we write $Z_j = Z(\mathrm{lon}_j, \mathrm{lat}_j, \mathrm{year}_j) = Y_{i_j} - u(\mathrm{lon}_{i_j}, \mathrm{lat}_{i_j})$ provided that $Y_{i_j} > u(\mathrm{lon}_{i_j}, \mathrm{lat}_{i_j})$ with the threshold $u(\mathrm{lon}_{i_j}, \mathrm{lat}_{i_j})$ set at location $(\mathrm{lon}_{i_j}, \mathrm{lat}_{i_j})$. The threshold $u(\mathrm{lon}_{i_j}, \mathrm{lat}_{i_j})$ was obtained as the 98%-quantile predicted with a generalized additive quantile regression approach that uses thin-plate spline (with basis dimension set to 50) to capture spatial variability. We report results for the models $M_k \sim \mathrm{GEV}(\mu_k, \sigma_k, \xi_k^{\mathrm{GEV}})$ and $Z_j \sim \mathrm{GP}(\tilde{\sigma}_j, \xi_j^{\mathrm{GP}})$ with the following generalized additive regression equations

(other results are provided in the online supplementary material):

$$\begin{aligned}
\mu(\text{lon}, \text{lat}, \text{year}) &= \mu_0 + s_\mu(\text{lon}, \text{lat}) + s_\mu(\text{year}), \\
\log \sigma(\text{lon}, \text{lat}, \text{year}) &= \sigma_0 + s_\sigma(\text{lon}, \text{lat}) + s_\sigma(\text{year}), \\
\xi^{\text{GEV}} &= \xi_0^{\text{GEV}}; \\
\log \tilde{\sigma}(\text{lon}, \text{lat}, \text{year}) &= \tilde{\sigma}_0 + s_{\tilde{\sigma}}(\text{lon}, \text{lat}) + s_{\tilde{\sigma}}(\text{year}), \\
\xi^{\text{GP}} &= \xi_0^{\text{GP}},
\end{aligned}$$

where spatial effects depending on (lon, lat) are implemented using thin-plate splines as for the quantile regression above and temporal effects depending on year are given by cubic regression splines (with basis dimension set to 10). It is noteworthy that the GAM framework is highly flexible and offers numerous other ways to include covariates in alternative model specifications. The GEV model has $21,648$ observations of maxima, whereas the GPD model uses $128,096$ observations of threshold excesses. All models could be fitted in less than a minute on a standard laptop computer.

Figure 1.3 shows spatial maps (top row) of estimated parameters (by fixing the year to 2023) and the estimated temporal trend (bottom row). The three parameters $\mu, \sigma, \tilde{\sigma}$ show relatively similar spatial and temporal patterns. Areas with higher elevations tend to have larger parameter estimates. The estimated partial temporal effect shows lower values at the beginning of the study period and around the year 1980. There is also a first peak around the year 1940 and a relatively strong increase towards unprecedented high values starting around the year 2000, which indicates the presence of some temporal trends during the study period. These trends could be due to slowly varying (but stationary) drivers of precipitation processes or could be a sign of temporal nonstationarity. Standard diagnostics for GAMs, such as confidence intervals, effective degrees of freedom of spline functions, and comparison of AIC values with simpler model variants, indicate that all of these trends are highly significant. Visually, the partial effects of the GPD scale $\tilde{\sigma}$ behave like a combination of the corresponding partial effects for the location μ and scale σ of the GEV distribution. This is not surprising since, by theory, the parameters are linked through $\tilde{\sigma} = \sigma + \xi(\mu - u)$, with ξ the tail index (here estimated to be roughly 0.15 in both GPD and GEV models), and u the location-dependent threshold used for the GPD.

The prediction of extreme quantiles is one of the standard uses of EVT-models and is illustrated with the spatial quantile maps (for the year 2023) in Figure 1.4. We have plotted a quantile at level 0.9 for annual maxima using the GEV fit. This value represents a ten-percent chance of being exceeded by the annual location-wise maximum of 2023. For the original event data, we plot a quantile at level $1 - 1/(10 \times 365)$, corresponding to a quantile at level 0.986 of the GP fit after taking into account the threshold exceedance probability of 0.02; this yields a value that had a ten-percent chance of being exceeded by any of the daily observations during the year 2023. Both maps can be interpreted as 10-year return levels under the assumption of a stationary climate. For

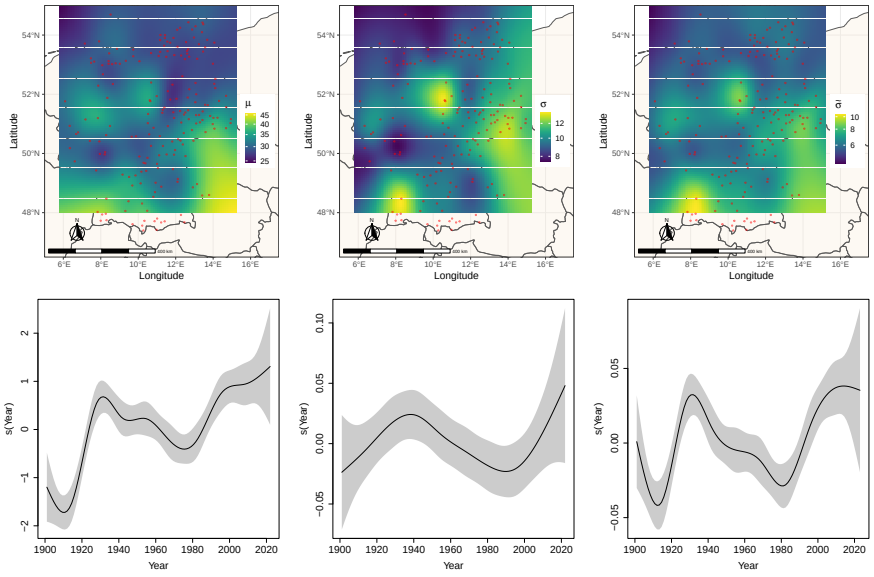

FIGURE 1.3
Estimated effects in the GAM models for German precipitation extremes with GEV and GP responses. Top row: Estimated spatial parameter surfaces (from left to right) for $\mu(\text{lon}, \text{lat})$ and $\sigma(\text{lon}, \text{lat})$ with the GEV model and $\tilde{\sigma}(\text{lon}, \text{lat})$ with the GP model. Bottom row: Estimated temporal trend component (from left to right) $s_\mu(\text{year})$, $s_\sigma(\text{year})$ and $s_{\tilde{\sigma}}(\text{year})$, here with confidence intervals based on standard `evgam` output.

the GP-based quantile map, we have added the threshold predicted by the quantile regression to the GP quantile in order to obtain a predicted quantile for the original events. The spatial patterns and the average quantile levels of GEV and GP predictions are quite similar, but the GP quantile map shows slightly stronger spatial variability. This is possibly due to the larger number of observed threshold exceedances by comparison with the number of observed maxima, such that GP data provide more information, leading to less spatial smoothing.

1.7 Towards stochastic weather generator models

Numerical climate models have severe limitations and potential biases in simulating large numbers of realizations of precipitation fields (especially rain-

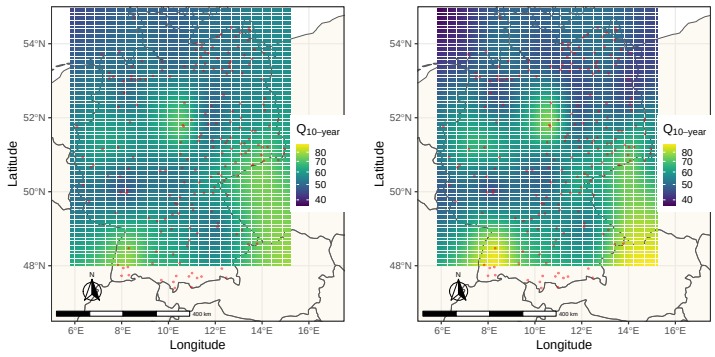

FIGURE 1.4
Maps of predicted high quantiles for precipitation extremes in 2023 with GEV (left display) and GP responses (right display). Both quantile maps can be interpreted as 10-year return levels. Left map: GEV-quantile at level 0.9. Right map: GP-quantile, with the threshold added, at level 0.986.

fall) with desired statistical properties. An interesting alternative is the use of stochastic rainfall generators to generate synthetic but realistic rainfall episodes, including dry sequences. Emulators are specific variants of generators that aim to reproduce climate model output and its key statistical properties as faithfully as possible but at a much lower cost. The parameters of generator models are usually statistically estimated from training data. The statistical properties of the episodes simulated by generator models are controlled to obtain the desired behavior in terms of rainfall variability, and a variety of geostatistical approaches, usually based on transformed Gaussian processes, have emerged [10].

Rainfall simulated by a generator can be used to conduct impact studies in various areas such as energy production, agronomy, and risk assessment. This generated rainfall can be used as input to a hydrological model for subsequent flood modeling and risk assessment. Simulators and emulators have practical applications beyond their primary use, such as evaluating numerical weather simulations or studying precipitation climatology.

Although many papers now broadly focus on the design of stochastic weather generators that also model the dependence between variables, the design of generators dedicated to rainfall remains a very active area of research. Rainfall is a key variable of the climate system and critical for many applications; the design of generators that account for its complexity poses many challenges, and different families of methods have been proposed to address them. The purpose of this section is to present these approaches, using the methods and concepts introduced earlier in the chapter, with a focus on simulation purposes. The additional challenges associated with this specific

objective are discussed, and several references are provided for readers who wish to explore the topic further.

Some approaches are based on the principle of resampling [18, 90], such as the K-nearest neighbor algorithm, with which it is possible to combine perturbations to move away from the observed values. Other approaches rely on exogenous variables to add knowledge, often based on simulations using global climate models and are closely related to statistical downscaling techniques [78, 121, 122]. Similarly, precipitation generation based on weather types is an approach that relies on understanding the relationships between atmospheric conditions and precipitation patterns (see [1] for an overview).

The alternation of rainy and dry periods leads us to consider, in the simplest case, two states. These weather types can be further refined by dividing the type of precipitation into several subtypes, such as light rain, medium intensity rain, and heavy rain. The classification of weather types is based on the observation of several variables such as air pressure, temperature, humidity, wind speed, and direction. Each type of weather is associated with specific precipitation patterns, often taking into account local characteristics. For example, certain regions may have specific weather types associated with local weather phenomena such as Mediterranean events, monsoons, tropical storms, etc. Once the relationships between weather types and precipitation patterns are established, they are incorporated into the models, which then generate precipitation episodes based on the predicted weather types. While this method can provide satisfactory results in many situations, it has certain limitations. Atmospheric conditions can be complex and highly variable, and it can be difficult to capture all the nuances of precipitation patterns based on weather type classification alone.

An alternative to this *a priori* weather type identification approach is to consider the weather type as a latent variable, which is therefore not directly observable, in a Hidden Markov Model (HMM). The consideration of marginal distributions that are sufficiently flexible to be suitable for both regular and extreme events is also an interesting and increasingly used approach.

These aspects, discussed in detail in Chapter **??**, are of strong interest in precipitation modeling. The extended GP distribution [95, 83] takes advantage of the EVT for large and small positive values, providing a smooth, threshold-free transition between the upper and lower tails with a reasonable number of parameters. For example, based on the structure proposed by [120], [39] consider a two-state Markov chain (dry and wet) and combine it with an extended GP marginal distribution for the wet state. Specifically, [39] proposes a multi-site precipitation model that can account for temporal and spatial dependence in both the precipitation occurrence process and the precipitation intensity process. Their multi-site precipitation model shows good results and can be combined with temporal disaggregation to obtain sub-daily data, as shown in [113] with weather analogs.

The concept of censoring a Gaussian vector or process is a flexible tool for precipitation modeling. It provides a straightforward method for generating

the space-time evolution of binary variables. [2, 62] used this approach to model the occurrence of rainfall, allowing for effective handling of temporal and/or spatial dependence in the rain/non-rain alternation. In [2], the random variable modeling positive rain intensity is forced to zero for negative values. By design, this enables a high level of consistency in the relationship between light rain and no rain.

Modeling the spatial and temporal dependence structure is crucial for accurately reproducing positive values. Gaussian processes are a suitable option for this purpose, as previously discussed. Another option is to use models based on cylinders in space-time, such as those presented by [98] and [28], where the cylinders represent rain cells grouped in clusters. However, these models are not suitable for extreme values.

For the study of spatial extremes, max-stable processes are the natural spatial extension for modeling maxima (see Chapter **??** in this book), and in 2002 [104] introduced spatial max-stable processes with random set elements. [56] extended this concept by fitting a space-time version to threshold exceedances of hourly rainfall data using pairwise censored likelihood. In their approach, storms are modeled as discs of random radius moving at random velocities for random durations, involving randomly centered space-time cylinders. However, one of their drawbacks is the difficulty in interpreting the fields simulated by these models at the event scale.

[43] extended the POT approach based on the GP distribution to the infinite-dimensional case by introducing Pareto processes (see Chapter **??** in this book). The condition is based on supremum exceedances over the study area. To gain flexibility, [37, 31, 32] consider the notion of ℓ-Pareto processes by considering more general exceedances defined for a homogeneous cost function denoted ℓ. Following [31], we can also talk about the risk functional, as it determines the type of extreme events whose risk we want to study. The authors propose an application to rainfall in Florida, which they carry out using different examples of functional that allow us to consider different types of rainfall (local and intense, or accumulation of rain spread over space).

Following the formalism of Pareto processes extended to the spatio-temporal framework, [93] propose a semi-parametric approach for simulating extreme spatio-temporal episodes. The approach is based on resampling for the dependence structure and on the univariate theory of extremes for marginal modeling. The framework of max-stable and ℓ-Pareto processes is based on the hypothesis of asymptotic dependence. These models assume that the dependence remains constant regardless of the extreme level considered. However, they are not suitable for situations of asymptotic independence (AI), where the strength of the dependence decreases as the extreme level considered increases until it disappears at the limit. Although difficult to identify in practice, this situation appears to occur for precipitation data (see [29, 69, 107]). This is also the case for the hourly data in southern France studied in [4]. Based on the same geometric objects as [56], slated cylinders, they propose a space-time modeling of exceedances that leads to asymptotic independence in space and

time. This is a hierarchical approach involving a space-time gamma process convolution in the rate of an exponential variable. The dependence structure is anisotropic, and nonstationarity of the dependence structure is possible in the model but would complicate parameter inference. One of the strengths of this approach is the physical interpretation of the parameters. Other very recent approaches free themselves from any parametric form using methods from generative artificial intelligence such as generative adversarial networks [14]. Other methods such as variational autoencoders have also recently been used in [66] in a multivariate framework to generate multivariate extremes (see also [126]).

When generating precipitation over a large area with nonstationarity, it is ideal to consider independent zones, at least for extreme events. Using one model per zone would prevent models with too many parameters, but the important question remains how to create these clusters. One way is to perform spatial clustering of precipitation data based on the extreme dependence present in the data. [11] performed such a clustering on weekly rainfall data in France using the PAM algorithm on extremal dependence. [102] uses the same idea and shows an interest in using a hierarchical clustering algorithm. Based on the recent development of an algorithm specifically tailored for AI block models [16], the authors propose in [15] a spatial clustering method of temporal processes adapted to the occurrence of two extreme events occurring simultaneously. They propose a regionalization of Europe based on daily precipitation amounts and daily maximum wind speed data from the ERA5 reanalysis dataset from 1979 to 2022. Another clustering method for compound extremes in several variables has been proposed by [112], but it is not based on the deviation from AI, but on the differences in the distribution, as it is based on the Kullback-Leibler divergence.

1.8 Conclusions and perspectives

Precipitation, and especially rainfall, is a complex hydrometeorological phenomenon. It is intermittent by nature, which must be taken into account in models, and its behavior depends on the temporal and spatial aggregation considered, which must also be taken into account. The modeling of rainfall data is a highly interdisciplinary exercise, which is the subject of intense research in various journals in fields such as statistics, hydrology, and climate. The large number of bibliographic entries in this chapter, extracted by several subject categories but still representing only a very small fraction of the relevant literature, illustrates this fact. Extreme precipitation events pose a challenge because of the variety of types of events that fall under this definition. The simulation of rainfall series that seamlessly include extreme rainfall events is an exciting and very challenging area of research.

Modeling the spatial and temporal dependence structure of extremes is a significant challenge. Suggesting a flexible dependence structure can be difficult because different types of dependence, such as asymptotic dependence or independence, are required depending on which dimension (spatial or temporal) we consider [116, 5, 57, 64, 58, 13]. Additionally, the problem of spatial nonstationarity of the spatial dependency structure arises, as even small spatial scales can exhibit complex topographies. Nonstationarity can also be temporal, where identifying and modeling differences in dependency structures over time can be challenging. In addition to these issues related to modeling extreme dependence, we encounter other difficulties when attempting to model bulk and extreme precipitation simultaneously. While marginal modeling of bulk and extreme rainfall is well covered in the literature, flexible and adaptive modeling to ensure transitions in the dependence structure associated with rainfall is largely unexplored [3].

As mentioned earlier, artificial intelligence (AI) approaches have the potential to address complex modeling problems, such as stochastic space-time precipitation generators, see [40] for a general overview of the potential benefits of machine learning and AI in the climate domain. However, AI-based generators may face challenges in accurately controlling and replicating all relevant precipitation characteristics in the generated data. To improve precipitation generators, a promising approach is to combine artificial intelligence with knowledge from extreme value theory and the physics of the hydrometeorological process under study. It is generally recommended to use methods that integrate both the physics of the phenomena and statistical methods when directly modeling floods, a natural disaster that can cause significant damage and remains difficult to predict at short time horizons. With climate change and urbanization, floods are expected to become more frequent and severe. The costs associated with flooding also increase due to changes in insured exposures, and flood risk assessment involves a wide range of considerations, with statistical analysis of extreme precipitation events at its core.

Acknowledgement

We are indebted to Ilaria Prosdocimi for valuable suggestions on some bibliographic references and for pointing out the existence of some relevant R packages.

Bibliography

[1] Pierre Ailliot, Denis Allard, Valérie Monbet, and Philippe Naveau. Stochastic weather generators: an overview of weather type models. *Journal de la Société Française de Statistique*, 156(1):101–113, 2015.

[2] Denis Allard and Marc Bourotte. Disaggregating daily precipitations into hourly values with a transformed censored latent Gaussian process. *Stochastic Environmental Research and Risk Assessment*, 29:453–462, 2015.

[3] Lídia Maria André, Jennifer L Wadsworth, and Adrian O'Hagan. Joint modelling of the body and tail of bivariate data. *Computational Statistics & Data Analysis*, 189:107841, 2024.

[4] Jean-Noël Bacro, Carlo Gaetan, Thomas Opitz, and Gwladys Toulemonde. Hierarchical space-time modeling of asymptotically independent exceedances with an application to precipitation data. *Journal of the American Statistical Association*, 115(530):555–569, 2020.

[5] Jean-Noël Bacro, Carlo Gaetan, and Gwladys Toulemonde. A flexible dependence model for spatial extremes. *Journal of Statistical Planning and Inference*, 172:36–52, 2016.

[6] August A Balkema and Laurens De Haan. Residual life time at great age. *Annals of Probability*, 2(5):792–804, 1974.

[7] Aurelien Bechler, Mathieu Vrac, and Liliane Bel. A spatial hybrid approach for downscaling of extreme precipitation fields. *Journal of Geophysical Research: Atmospheres*, 120(10):4534–4550, 2015.

[8] Jan Beirlant, Yuri Goegebeur, Johan Segers, and Jozef Teugels. *Statistics of Extremes: Theory and Applications*. John Wiley & Sons, New York, 2004.

[9] Léo R Belzile, Christophe Dutang, Paul J Northrop, and Thomas Opitz. A modeler's guide to extreme value software. *Extremes*, pages 1–44, 2023.

[10] Lionel Benoit and Gregoire Mariethoz. Generating synthetic rainfall with geostatistical simulations. *Wiley Interdisciplinary Reviews: Water*, 4(2):e1199, 2017.

[11] Elsa Bernard, Philippe Naveau, Mathieu Vrac, and Olivier Mestre. Clustering of maxima: spatial dependencies among heavy rainfall in France. *Journal of Climate*, 26(20):7929 – 7937, 2013.

[12] Juliette Blanchet, Davide Ceresetti, Gilles Molinié, and Jean-Dominique Creutin. A regional GEV scale-invariant framework for Intensity–Duration–Frequency analysis. *Journal of Hydrology*, 540:82–95, 2016.

[13] Paola Bortot and Carlo Gaetan. A model for space-time threshold exceedances with an application to extreme rainfall. *Statistical Modelling*, 24(2):169–193, 2024.

[14] Younes Boulaguiem, Jakob Zscheischler, Edoardo Vignotto, Karin van der Wiel, and Sebastian Engelke. Modeling and simulating spatial extremes by combining extreme value theory with generative adversarial networks. *Environmental Data Science*, 1:e5, 2022.

[15] Alexis Boulin, Elena Di Bernardino, Thomas Laloë, and Gwladys Toulemonde. Identifying regions of concomitant compound precipitation and wind speed extremes over Europe. *arXiv:2311.11292*, 2023.

[16] Alexis Boulin, Elena Di Bernardino, Thomas Laloë, and Gwladys Toulemonde. High-dimensional variable clustering based on sub-asymptotic maxima of a weakly dependent random process. *arXiv: 2302.00934*, 2023.

[17] Bruce M. Brown and Sidney I. Resnick. Extreme values of independent stochastic processes. *Journal of Applied Probability*, 14(4):732–739, 1977.

[18] T. Adri Buishand. Extreme rainfall estimation by combining data from several sites. *Hydrological Sciences Journal*, 36(4):345–365, 1991.

[19] Julie Carreau and Gwladys Toulemonde. Extra-parametrized extreme value copula: extension to a spatial framework. *Spatial Statistics*, 40, 2020.

[20] Daniela Castro-Camilo and Raphaël Huser. Local likelihood estimation of complex tail dependence structures, applied to US precipitation extremes. *Journal of the American Statistical Association*, 115(531):1037–1054, 2020.

[21] Richard E Chandler and Steven Bate. Inference for clustered data using the independence loglikelihood. *Biometrika*, 94(1):167–183, 2007.

[22] Valérie Chavez-Demoulin and Anthony C. Davison. Generalized additive modelling of sample extremes. *Journal of the Royal Statistical Society, Series C*, 54(1):207–222, 2005.

[23] Ying Ruan Chen and Pao-Shin Chu. Trends in precipitation extremes and return levels in the Hawaiian islands under a changing climate. *International Journal of Climatology*, 34(15):3913–3925, 2014.

[24] Stuart G. Coles. *An Introduction to Statistical Modeling of Extreme Value*. Springer, London, 2001.

[25] Stuart G. Coles and Mark J. Dixon. Likelihood-based inference for extreme value models. *Extremes*, 2(1):5–23, 1999.

[26] Daniel Cooley, Douglas Nychka, and Philippe Naveau. Bayesian spatial modeling of extreme precipitation return levels. *Journal of the American Statistical Association*, 102(479):824–840, 2007.

[27] Daniel Cooley and Stephan R. Sain. Spatial hierarchical modeling of precipitation extremes from a regional climate model. *Journal of Agricultural, Biological, and Environmental Statistics*, 15:381–402, 2010.

[28] David Roxbee Cox and Valerie Isham. A simple spatial-temporal model of rainfall. *Proceedings of the Royal Society of London. A. Mathematical and Physical Sciences*, 415(1849):317–328, 1988.

[29] Anthony C. Davison, Raphaël Hüser, and Emeric Thibaud. Geostatistics of dependent and asymptotically independent extremes. *Mathematical Geosciences*, 45:511–529, 2013.

[30] Anthony C. Davison and Richard L. Smith. Models for exceedances over high thresholds. *Journal of the Royal Statistical Society, Series B*, 52(3):393–425, 1990.

[31] Raphaël de Fondeville and Anthony C. Davison. High-dimensional peaks-over-threshold inference. *Biometrika*, 105(3):575–592, 06 2018.

[32] Raphaël de Fondeville and Anthony C. Davison. Functional peaks-over-threshold analysis. *Journal of the Royal Statistical Society, Series B*, 84(4):1392–1422, 2022.

[33] Laurens de Haan and Ana Ferreira. *Extreme Value Theory: an Introduction*. Springer, New York, 2006.

[34] Johannes de Leeuw, John Methven, and Michael Blackburn. Evaluation of ERA-Interim reanalysis precipitation products using England and Wales observations. *Quarterly Journal of the Royal Meteorological Society*, 141(688):798–806, 2015.

[35] Carlo De Michele and Francesco Avanzi. Superstatistical distribution of daily precipitation extremes: A worldwide assessment. *Scientific Reports*, 8(1), 2018.

[36] Tufa Dinku, Kinfe Hailemariam, Ross Maidment, Elena Tarnavsky, and Stephen Connor. Combined use of satellite estimates and rain gauge observations to generate high-quality historical rainfall time series over ethiopia. *International Journal of Climatology*, 34(7):2489–2504, 2013.

[37] Clément Dombry and Mathieu Ribatet. Functional regular variations, pareto processes and peaks over threshold. *Statistics and Its Interface*, 8(1):9–17, 2015.

[38] Shannon Doocy, Amy Daniels, Sarah Murray, and Thomas D Kirsch. The human impact of floods: a historical review of events 1980-2009 and systematic literature review. *PLoS Currents*, 5(5), 2013.

[39] Guillaume Evin, Anne-Catherine Favre, and Benoît Hingray. Stochastic generation of multi-site daily precipitation focusing on extreme events. *Hydrology and Earth System Sciences*, 22(1):655–672, 2018.

[40] Veronika Eyring, William D Collins, Pierre Gentine, Elizabeth A Barnes, Marcelo Barreiro, Tom Beucler, Marc Bocquet, Christopher S Bretherton, Hannah M Christensen, Katherine Dagon, et al. Pushing the frontiers in climate modelling and analysis with machine learning. *Nature Climate Change*, pages 1–13, 2024.

[41] Felix S. Fauer, Jana Ulrich, Oscar E. Jurado, and Henning W. Rust. Flexible and consistent quantile estimation for intensity–duration–frequency curves. *Hydrology and Earth System Sciences*, 25(12):6479–6494, 2021.

[42] Lee Fawcett and David Walshaw. Improved estimation for temporally clustered extremes. *Environmetrics*, 18(2):173–188, 2007.

[43] Ana Ferreira and Laurens de Haan. The generalized Pareto process; with a view towards application and simulation. *Bernoulli*, 20(4):1717 – 1737, 2014.

[44] Christopher A. T. Ferro and Johan Segers. Inference for clusters of extreme values. *Journal of the Royal Statistical Society, Series B*, 65(2):545–556, 2003.

[45] Ronald Aylmer Fisher and Leonard Henry Caleb Tippett. Limiting forms of the frequency distribution of the largest or smallest member of a sample. *Mathematical Proceedings of the Cambridge Philosophical Society*, 24(2):180–190, 1928.

[46] Hayley J. Fowler, Geert Lenderink, Andreas F. Prein, Seth Westra, Richard P. Allan, Nikolina Ban, Renaud Barbero, Peter Berg, Stephen Blenkinsop, Hong X Do, et al. Anthropogenic intensification of short-duration rainfall extremes. *Nature Reviews Earth & Environment*, 2(2):107–122, 2021.

[47] Petra Friederichs. Statistical downscaling of extreme precipitation events using extreme value theory. *Extremes*, 13:109–132, 2010.

[48] Reinhard Furrer and Philippe Naveau. Probability weighted moments properties for small samples. *Statistics & Probability Letters*, 77(2):190–195, 2007.

[49] Boris Vladimirovich Gnedenko. Sur la distribution limite du terme maximum d'une série aléatoire. *Annals of Mathematics*, 44(3):423–453, July 1943.

[50] Joseph A. Greenwood, Jurate M. Landwehr, Nicolas C. Matalas, and James R Wallis. Probability weighted moments: definition and relation to parameters of several distributions expressable in inverse form. *Water Resources Research*, 15(5):1049–1054, 1979.

[51] Abubakar Haruna, Juliette Blanchet, and Anne-Catherine Favre. Modeling intensity-duration-frequency curves for the whole range of nonzero precipitation: A comparison of models. *Water Resources Research*, 59(6):e2022WR033362, 2023.

[52] Arnab Hazra, Raphaël Huser, and Árni V Jóhannesson. Bayesian latent Gaussian models for high-dimensional spatial extremes. In *Statistical Modeling Using Bayesian Latent Gaussian Models: With Applications in Geophysics and Environmental Sciences*, pages 219–251. Springer, 2023.

[53] Jonathan R. M. Hosking. L-moments: Analysis and estimation of distributions using linear combinations of order statistics. *Journal of the Royal Statistical Society, Series B*, 52(1):105–124, 1990.

[54] Jonathan R. M. Hosking and James R Wallis. *Regional Frequency Analysis: An Approach Based on L-Moments*. Cambridge University Press, Cambridge, UK, 1997.

[55] Jonathan R. M. Hosking, James R. Wallis, and Eric F. Wood. Estimation of the generalized extreme-value distribution by the method of probability-weighted moments. *Technometrics*, 27(3):251–261, 1985.

[56] Raphaël Huser and Anthony C. Davison. Space—time modelling of extreme events. *Journal of the Royal Statistical Society, Series B*, pages 439–461, 2014.

[57] Raphaël Huser, Thomas Opitz, and Emeric Thibaud. Bridging asymptotic independence and dependence in spatial extremes using Gaussian scale mixtures. *Spatial Statistics*, 21:166–186, 2017.

[58] Raphaël Huser and Jennifer L. Wadsworth. Modeling Spatial Processes with Unknown Extremal Dependence Class. *Journal of the American Statistical Association*, 114(525):434–444, 2019.

[59] Arthur F. Jenkinson. The frequency distribution of the annual maximum (or minimum) values of meteorological elements. *Quarterly Journal of the Royal Meteorological Society*, 81(348):158–171, 1955.

[60] Fei Ji, Giovanni Di Virgilio, Nidhi Nishant, Eugene Tam, Jason P. Evans, Jatin Kala, Julia Andrys, Chris Thomas, and Matthew L. Riley. Evaluation of precipitation extremes in ERA5 reanalysis driven regional climate simulations over the CORDEX-Australasia domain. *Weather and Climate Extremes*, 44:100676, 2024.

[61] Viatcheslav V. Kharin, Francis W. Zwiers, Xuebin Zhang, and Gabriele C. Hegerl. Changes in temperature and precipitation extremes in the IPCC ensemble of global coupled model simulations. *Journal of Climate*, 20(8):1419–1444, 2007.

[62] William Kleiber, Richard W. Katz, and Balaji Rajagopalan. Daily spatiotemporal precipitation simulation using latent and transformed Gaussian processes. *Water Resources Research*, 48(1), 2012.

[63] Demetris Koutsoyiannis, Demosthenes Kozonis, and Alexandros Manetas. A mathematical framework for studying rainfall intensity-duration-frequency relationships. *Journal of Hydrology*, 206(1):118–135, 1998.

[64] Pavel Krupskii and Marc G. Genton. Factor copula models for data with spatio-temporal dependence. *Spatial Statistics*, 22:180–195, 2017.

[65] Zbigniew W. Kundzewicz and Alice J. Robson. Change detection in hydrological records – a review of the methodology. *Hydrological Sciences Journal*, 49(1):7–19, 2004.

[66] Nicolas Lafon, Philippe Naveau, and Ronan Fablet. A VAE approach to sample multivariate extremes. *arXiv:2306.10987*, 2023.

[67] Jurate M. Landwehr, Nicolas C. Matalas, and James R. Wallis. Probability weighted moments: definition and relation to parameters of several distributions expressable in inverse form. *Water Resources Research*, 15:1049–1054, 1979.

[68] Andreas Langousis, Antonios Mamalakis, Michelangelo Puliga, and Roberto Deidda. Threshold detection for the generalized Pareto distribution: Review of representative methods and application to the NOAA NCDC daily rainfall database. *Water Resources Research*, 52(4):2659–2681, 2016.

[69] Phuong Dong Le, Anthony C. Davison, Sebastian Engelke, Michael Leonard, and Seth Westra. Dependence properties of spatial rainfall extremes and areal reduction factors. *Journal of Hydrology*, 565:711–719, 2018.

[70] Philomène Le Gall, Anne-Catherine Favre, Philippe Naveau, and Clèmentine Prieur. Improved regional frequency analysis of rainfall data. *Weather and Climate Extremes*, 36:100456, 2022.

[71] Geert Lenderink, Renaud Barbero, Jessica M. Loriaux, and Hayley J. Fowler. Super-Clausius–Clapeyron scaling of extreme hourly convective precipitation and its relation to large-scale atmospheric conditions. *Journal of Climate*, 30(15):6037–6052, 2017.

[72] Geert Lenderink and Erik Van Meijgaard. Increase in hourly precipitation extremes beyond expectations from temperature changes. *Nature Geoscience*, 1(8):511–514, 2008.

[73] Ming Li and Quanxi Shao. An improved statistical approach to merge satellite rainfall estimates and raingauge data. *Journal of Hydrology*, 385(1–4):51–64, 2010.

[74] Shaw Chen Liu, Congbin Fu, Chein-Jung Shiu, Jen-Ping Chen, and Futing Wu. Temperature dependence of global precipitation extremes. *Geophysical Research Letters*, 36(17), 2009.

[75] Robert E. Livezey and Wilbur Y. Chen. Statistical field significance and its determination by Monte Carlo techniques. *Monthly Weather Review*, 111(1):46–59, 1983.

[76] Henry B. Mann. Nonparametric tests against trend. *Econometrica*, 13(3):245–259, 1945.

[77] Marco Marani and Massimiliano Ignaccolo. A metastatistical approach to rainfall extremes. *Advances in Water Resources*, 79:121–126, 2015.

[78] Douglas Maraun, Frederick Wetterhall, Anderson M. Ireson, Richard E. Chandler, Elizabeth J. Kendon, Martin Widmann, S. Brienen, Henning W. Rust, Tobias Sauter, Matthias Themeßl, Victor K. C. Venema, Kwok P. Chun, C. M. Goodess, Richard G. Jones, Christian Onof, Mathieu Vrac, and Insa Thiele-Eich. Precipitation downscaling under climate change: Recent developments to bridge the gap between dynamical models and the end user. *Reviews of Geophysics*, 48(3), 2010.

[79] Cristian Martinez-Villalobos and J. David Neelin. Why do precipitation intensities tend to follow gamma distributions? *Journal of the Atmospheric Sciences*, 76(11):3611–3631, 2019.

[80] Giuseppe Mascaro. Comparison of local, regional, and scaling models for rainfall intensity–duration–frequency analysis. *Journal of Applied Meteorology and Climatology*, 59(9):1519–1536, 2020.

[81] Conor Murphy, Jonathan A. Tawn, and Zak Varty. Automated threshold selection and associated inference uncertainty for univariate extremes. *arXiv:2310.17999*, 2023.

[82] Saralees Nadarajah, Clive W. Anderson, and Jonathan A. Tawn. Ordered multivariate extremes. *Journal of the Royal Statistical Society, Series B*, 60(2):473–496, 1998.

[83] Philippe Naveau, Raphaël Huser, Pierre Ribereau, and Alexis Hannart. Modeling jointly low, moderate, and heavy rainfall intensities without a threshold selection. *Water Resources Research*, 52(4):2753–2769, 2016.

[84] Sofia D. Nerantzaki and Simon Michael Papalexiou. Assessing extremes in hydroclimatology: A review on probabilistic methods. *Journal of Hydrology*, 605:127302, 2022.

[85] Katrin M Nissen and Uwe Ulbrich. Increasing frequencies and changing characteristics of heavy precipitation events threatening infrastructure in Europe under climate change. *Natural Hazards and Earth System Sciences*, 17(7):1177–1190, 2017.

[86] Paul J. Northrop, Nicolas Attalides, and Philip Jonathan. Cross-validatory extreme value threshold selection and uncertainty with application to ocean storm severity. *Journal of the Royal Statistical Society, Series C*, 66(1):93–120, 2017.

[87] Marco Oesting, Liliane Bel, and Christian Lantuéjoul. Sampling from a max-stable process conditional on a homogeneous functional with an application for downscaling climate data. *Scandinavian Journal of Statistics*, 45(2):382–404, 2018.

[88] Helga K. Olafsdottir, Holger Rootzén, and David Bolin. Extreme rainfall events in the Northeastern United States become more frequent with rising temperatures, but their intensity distribution remains stable. *Journal of Climate*, 34(22):8863–8877, 2021.

[89] Thomas Opitz, Raphaël Huser, Haakon Bakka, and Håvard Rue. INLA goes extreme: Bayesian tail regression for the estimation of high spatio-temporal quantiles. *Extremes*, 21(3):441–462, 2018.

[90] Fabio Oriani, Julien Straubhaar, Philippe Renard, and Gregoire Mariethoz. Simulation of rainfall time series from different climatic regions using the direct sampling technique. *Hydrology and Earth System Sciences*, 18(8):3015–3031, 2014.

[91] Taha B.M.J. Ouarda, Latifa A. Yousef, and Christian Charron. Non-stationary intensity-duration-frequency curves integrating information concerning teleconnections and climate change. *International Journal of Climatology*, 39(4):2306–2323, 2019.

[92] Paul A O'Gorman. Precipitation extremes under climate change. *Current Climate Change Reports*, 1:49–59, 2015.

[93] Fatima Palacios Rodriguez, Gwladys Toulemonde, Julie Carreau, and Thomas Opitz. Generalized Pareto processes for simulating space-time extreme events: an application to precipitation reanalyses. *Stochastic Environmental Research and Risk Assessment*, 34:2033–2052, 2020.

[94] Simon Michael Papalexiou and Demetris Koutsoyiannis. Battle of extreme value distributions: A global survey on extreme daily rainfall. *Water Resources Research*, 49(1):187–201, 2013.

[95] Ioannis Papastathopoulos and Jonathan A. Tawn. Extended generalised Pareto models for tail estimation. *Journal of Statistical Planning and Inference*, 143(1):131–143, 2013.

[96] James Pickands III. Statistical inference using extreme order statistics. *The Annals of Statistics*, 3(1):119 – 131, 1975.

[97] Philip Prescott and Andrew T. Walden. Maximum likelihood estimation of the parameters of the three-parameter generalized extreme-value distribution from censored samples. *Journal of Statistical Computation and Simulation*, 16:241–250, 1983.

[98] Ignacio Rodriguez-Iturbe, David R. Cox, and Valerie Isham. Some models for rainfall based on stochastic point processes. *Proceedings of the Royal Society of London. A. Mathematical and Physical Sciences*, 410(1839):269–288, 1987.

[99] Cynthia Rosenzweig, Francesco N Tubiello, Richard Goldberg, Evan Mills, and Janine Bloomfield. Increased crop damage in the US from excess precipitation under climate change. *Global Environmental Change*, 12(3):197–202, 2002.

[100] Huiyan Sang and Alan E Gelfand. Hierarchical modeling for extreme values observed over space and time. *Environmental and Ecological Statistics*, 16(3):407–426, 2009.

[101] Huiyan Sang and Alan E Gelfand. Continuous spatial process models for spatial extreme values. *Journal of Agricultural, Biological, and Environmental Statistics*, 15:49–65, 2010.

[102] Kate R. Saunders, Alec G. Stephenson, and David J. Karoly. A regionalisation approach for rainfall based on extremal dependence. *Extremes*, 24:215–240, 2021.

[103] Carl Scarrott and Anna MacDonald. A review of extreme value threshold estimation and uncertainty quantification. *REVSTAT-Statistical Journal*, 10(1):33–60, 2012.

[104] Martin Schlather. Models for stationary max-stable random fields. *Extremes*, 5:33–44, 2002.

[105] Richard L. Smith. Regional estimation from spatially dependent data. *Preprint. https://rls.sites.oasis.unc.edu/postscript/rs/regest.pdf*, 1990.

[106] Cecilia Svensson and David A. Jones. Review of rainfall frequency estimation methods. *Journal of Flood Risk Management*, 3(4):296–313, 2010.

[107] Emeric Thibaud, Raphaël Mutzner, and Anthony C Davison. Threshold modeling of extreme spatial rainfall. *Water Resources Research*, 49(8):4633–4644, 2013.

[108] Clement Tisseuil, Mathieu Vrac, Sovan Lek, and Andrew J. Wade. Statistical downscaling of river flows. *Journal of Hydrology*, 385(1):279–291, 2010.

[109] Hristos Tyralis and Andreas Langousis. Estimation of intensity–duration–frequency curves using max-stable processes. *Stochastic Environmental Research and Risk Assessment*, 33(1):239–252, 2019.

[110] Daniele Veneziano, Andreas Langousis, and Chiara Lepore. New asymptotic and preasymptotic results on rainfall maxima from multifractal theory. *Water Resources Research*, 45(11), 2009.

[111] Daniele Veneziano and Seonkyoo Yoon. Rainfall extremes, excesses, and intensity-duration-frequency curves: A unified asymptotic framework and new nonasymptotic results based on multifractal measures. *Water Resources Research*, 49(7):4320–4334, 2013.

[112] Edoardo Vignotto, Sebastian Engelke, and Jakob Zscheischler. Clustering bivariate dependencies of compound precipitation and wind extremes over Great Britain and Ireland. *Weather and Climate Extremes*, 32:100318, 2021.

[113] Daniele Viviroli, A. E. Sikorska-Senoner, Guillaume Evin, Maria Staudinger, Martina Kauzlaric, Jeremy Chardon, Anne-Catherine. Favre, Benoît Hingray, Gilles Nicolet, Damien Raynaud, Jan Seibert, ROlf Weingartner, and Calvin Whealton. Comprehensive space–time hydrometeorological simulations for estimating very rare floods at multiple sites in a large river basin. *Natural Hazards and Earth System Sciences*, 22(9):2891–2920, 2022.

[114] Richard E. von Mises. La distribution de la plus grande de n valeurs. *Revue Mathématique de l'Union Interbalcanique*, 1:141–160, 1936.

[115] Jennifer L. Wadsworth. Exploiting structure of maximum likelihood estimators for extreme value threshold selection. *Technometrics*, 58(1):116–126, 2016.

[116] Jennifer L. Wadsworth and Jonathan A. Tawn. Dependence modelling for spatial extremes. *Biometrika*, 99(2):253–272, 2012.

[117] Quan J. Wang. The POT model described by the generalized Pareto distribution with Poisson arrival rate. *Journal of Hydrology*, 129(1):263–280, 1991.

[118] Conrad Wasko and Ashish Sharma. Quantile regression for investigating scaling of extreme precipitation with temperature. *Water Resources Research*, 50(4):3608–3614, 2014.

[119] Seth Westra and Scott A Sisson. Detection of non-stationarity in precipitation extremes using a max-stable process model. *Journal of Hydrology*, 406(1-2):119–128, 2011.

[120] Daniel S. Wilks. Multisite generalization of a daily stochastic precipitation generation model. *Journal of Hydrology*, 210(1):178–191, 1998.

[121] Daniel S. Wilks. Use of stochastic weather generators for precipitation downscaling. *WIREs Climate Change*, 1(6):898–907, 2010.

[122] Daniel S. Wilks. Stochastic weather generators for climate-change downscaling, part II: multivariable and spatially coherent multisite downscaling. *WIREs Climate Change*, 3(3):267–278, 2012.

[123] Benjamin D. Youngman. evgam: An R Package for Generalized Additive Extreme Value Models. *Journal of Statistical Software*, 103(3):1–26, 2022.

[124] Sheng Yue and Chun Yuan Wang. Applicability of prewhitening to eliminate the influence of serial correlation on the Mann–Kendall test. *Water Resources Research*, 38(6):4–1, 2002.

[125] Joel Zeder and Erich M Fischer. Observed extreme precipitation trends and scaling in Central Europe. *Weather and Climate Extremes*, 29:100266, 2020.

[126] Likun Zhang, Xiaoyu Ma, Christopher K. Wikle, and Raphaël Huser. Flexible and efficient spatial extremes emulation via variational autoencoders. *ArXiv:2307.08079*, 2024.

[127] Qiang Zhang, Chong-Yu Xu, Zengxin Zhang, Yongqin David Chen, Chun-ling Liu, and Hui Lin. Spatial and temporal variability of precipitation maxima during 1960–2005 in the Yangtze River basin and possible association with large-scale circulation. *Journal of Hydrology*, 353(3-4):215–227, 2008.

[128] Peng Zhong, Manuela Brunner, Thomas Opitz, and Raphael Huser. Spatial modeling and future projection of extreme precipitation extents. *Journal of the American Statistical Association*, to appear, 2024.

[129] Enrico Zorzetto, Antonio Canale, and Marco Marani. A Bayesian non-asymptotic extreme value model for daily rainfall data. *Journal of Hydrology*, 628:130378, 2024.

Index

duration-dependent GEV
distribution, 13

Generalized Additive Model, 17
Generalized Logistic distribution, 8
Generalized Normal distribution, 8

Intensity-Duration-Frequency curves,
12

L-Moment, 11

Mann–Kendall test, 18
Metastatistical extreme value
distribution, 9

Pearson type III distribution, 8
Precipitation, 1
Probability Weighted Moment, 10

Regional Frequency Analysis, 15

statistical downscaling, 19
stochastic weather generator, 22